Metrol. Meas. Syst., Vol. XX (2013), No. 4, pp. 635–644.

PAN POLSKA AKADEMIA NAUK

METROLOGY AND MEASUREMENT SYSTEMS

Index 330930, ISSN 0860-8229

www.metrology.pg.gda.pl

M&MS

ANALYSIS OF NOISE AND NON-LINEARITY OF I-V CHARACTERISTICS OF POSITIVE TEMPERATURE COEFFICIENT CHIP THERMISTORS

Zdenek Sita[1)], Vlasta Sedlakova[2)], Jiri Majzner[2)], Petr Sedlak[2)], Josef Sikula[2)], Lubomir Grmela[2)]

1) *EPCOS s.r.o. Šumperk, Feritová 1, 78705 Šumperk, Czech Republic*
2) *Czech Noise Research Laboratory, Brno University of Technology, Faculty of Electrical Engineering and Communication, Department of Physics, Technicka 8, 616 00 Brno, Czech Republic (✉ sedlaka@feec.vutbr.cz, +420 54114 3398)*

Abstract

Noise spectroscopy and *I-V* characteristic non-linearity measurement were applied as diagnostic tools in order to characterize the volume and contact quality of positive temperature coefficient (PTC) chip sensors and to predict possible contact failure. Correctly made and stable contacts are crucial for proper sensing. *I-V* characteristics and time dependences of resistance were measured for studied sensors and, besides the samples with stable resistance value, spike type resistance fluctuation was observed for some samples. These spikes often disappear after about 24 hours of voltage application. Linear *I-V* characteristics were measured for the samples with stable resistance. The resistance fluctuation of burst noise type was observed for some samples showing the *I-V* characteristic dependent on the electric field orientation. We have found that the thermistors with high quality contacts had a linear *I-V* characteristic, the noise spectral density is of $1/f$ type and the third harmonic index is lower than 60 dB. The samples with poor quality contacts show non-linear *I-V* characteristics and excess noise is given by superposition of g-r and $1/f^n$ type noises, and the third harmonic index is higher than 60 dB.

Keywords: PTC chip sensors, noise spectroscopy, *I-V* characteristic non-linearity, quality evaluation.

1. Introduction

The method of quality analyses of positive temperature coefficient (PTC) chip temperature sensors by noise spectroscopy and *I-V* characteristic non-linearity evaluation is presented. A PTC thermistor is a thermally sensitive component with a positive temperature coefficient of resistance, which sharply increases with temperature after a defined temperature has been exceeded. The PTC thermistor is made of doped polycrystalline ceramics based on barium titanate, which is an insulating material. Semi-conductive properties are achieved by doping with higher valence atoms than those of the crystal lattice. PTC properties are achieved by the combination of ferroelectric properties of barium titanate and grain boundary barrier control. At the edges of the crystallites, called grain boundaries, potential barriers are created by controlled doping. The grain boundaries prevent free charge carriers to move between the grains, which results in high resistance. Heywang [1] describes the PTC behavior in terms of the enhanced height of the potential energy barrier with temperature, arising from the two-dimension layer of electron traps at grain boundaries. As an explanation for the resulting volume conductivity, a hopping model was proposed by Saburi [2], whereas Gerthsen et al [3] have presented a polaron charge carrier transport. A current transient with a peak was observed during the application of step voltage if a large charge is available at the injecting electrode (Zafar et al [4]). Undoped $BaTiO_3$ ceramics is an insulating material with resistivity higher than 10^{10} Ωcm at room temperature with a band gap of about 3 eV. The n-type conductivity is achieved by partial reduction of Ti^{4+}. In this case the additional electrons are not localized at room temperature and move in the electric field. Mobility is in the range

Article history: received on Mar. 26, 2013; accepted on Oct. 07, 2013; available online on Dec. 10, 2013; DOI: 10.2478/mms-2013-0054.

of 0.1 to 1 cm^2/Vs [5]. Oxygen vacancies and ions with higher valence can act also as donors with activation energy of the order of 0.1 eV [6].

Unreliability of electronic devices is caused predominantly by failures which result from the latent defects created during the manufacture processes or during the operating life of devices. A search for new non-destructive methods in order to characterize quality and predict reliability of vast ensembles became a trend in the last four decades. Charge carrier transport must be analyzed to understand stability and reliability of components and special attention must be paid to the contact between metal and semiconductor. Analyses of electron transport parameters are the most promising methods which provide non-destructive evaluation. Experiments are based on the measurements of device *I-V* characteristics [7], *I-V* characteristic nonlinearity using the non-linearity index (NLI) [8, 9], electronic noise spectroscopy [10 - 12], and electro-ultrasonic spectroscopy [13].

Noise spectroscopy and *I-V* characteristic non-linearity measurements are proposed as a diagnostic tool in order to characterize the sample bulk and contact quality, and to predict the mode of possible contact failure [14, 15]. These are sensitive techniques for analysis of bulk and interface defects for determining the quality of devices. Noise spectroscopy can be recommended rather for the technology evaluation due to the higher time demands for the realization of measurements, while the quick *I-V* characteristic non-linearity measurements can be used also as an on-line testing method.

2. Electron Transport Measurement

Correctly made and stable contacts are crucial for proper operation of PTC chip temperature sensors. High contact resistance could distort the temperature dependence of resistance towards lower value and influence the time behavior of the sensing levels of resistance. Namely microcracks and delaminations are seriously dangerous for the application, because the SMD chips are contacted to the printed circuit board by reflow or wave soldering, which creates high thermal shocks. Therefore the prediction methods of such failures, applicable to 100% of production tests, are of interest. The time dependence of the sensors resistance and the measurement of *I-V* characteristic are a basic method for quality evaluation. A stable resistance value and the *I-V* characteristic linear and symmetrical in both bias voltage orientations represent the minimal requirements for a high quality device.

2.1. Resistance vs. Time

Five ensembles of PTC thermistor samples denoted as STG1 and STG2 (electrodes made by technology G1 and G2), STB1, STB2, and M (electrodes made by technology B) were evaluated. The SMD limit temperature sensors of EIA STANDARD size 0402 (1 x 0.5 mm^2) were selected.

PTC chip thermistor parameters:

Maximum operating voltage:	32 V
Rated resistance @ 25°C:	540 ohm
Sensing temperature @4,7k ohm:	115°C

The SMD chips were soldered to the PCB by reflow soldering, using leadfree solder $SnAg_{3,5}Cu_{0,5}$ at peak temperature 245°C (see Fig. 1).

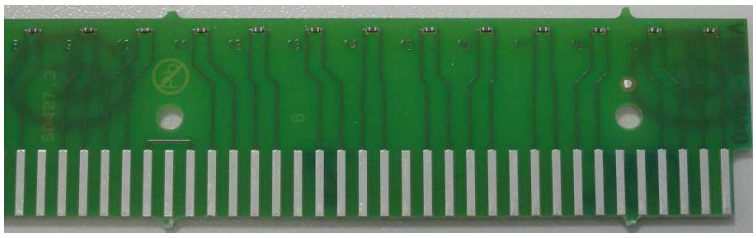

Fig. 1. SMD chips soldered to the PCB.

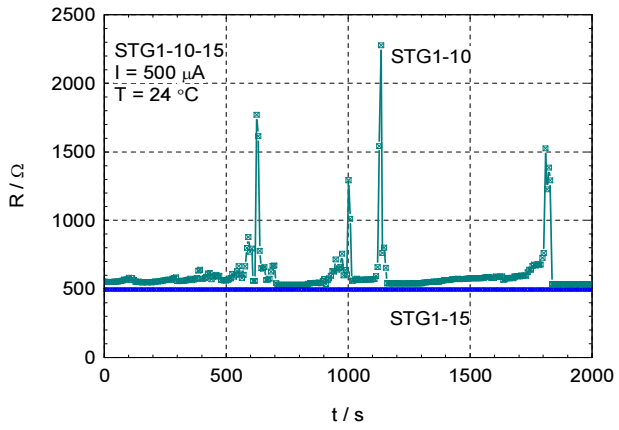

Fig. 2. Resistance vs. time for samples STG1-10 and STG1-15 for DC current I = 500 μA at a temperature of 24°C .

Time dependences of resistance for two samples of technology G: STG1-10 and STG1-15 for DC current I = 500 μA and T = 24°C are shown in Fig. 2. The sample STG1-15 has a stable resistance value R_0 = 490 Ω over time, whereas the resistance of sample STG1-10 reveals spikes. Spike-type resistance fluctuation was observed for some samples within each ensemble. These spikes are probably a result of the surface states, created by contaminating impurities, crystallographic defects, and lattice mismatching which unavoidably exist on the contact/active layer interface. These imperfections lead to the creation of filamentary carrier injection. The charge carrier transport has a stochastic component which often disappears after about 24 hours of voltage application.

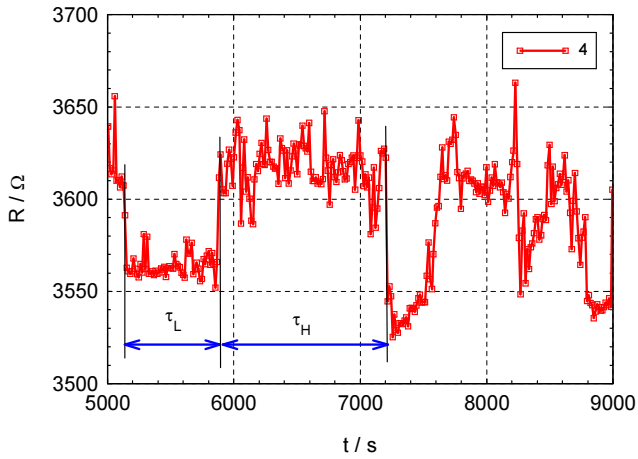

Fig. 3. Burst noise type resistance fluctuations measured for sample STB1-4 at T = 24°C .

For some samples, a resistance fluctuation of burst noise type was observed (see Fig. 3). These samples had a higher resistance value and often showed non-linear *I-V* characteristics.

2.2. I-V Characteristics

I-V characteristics were measured for the samples for both polarities of electric field; further denoted as measurements in normal mode – NM, and reverse mode – RM, respectively. The *I-V* characteristics measured for sample STG1-10, after the application of an 500 V/m electric field for 100 hours, is linear and symmetrical both in NM and RM as shown in Fig. 4. Here the resistance value R_0 = 503 Ω.

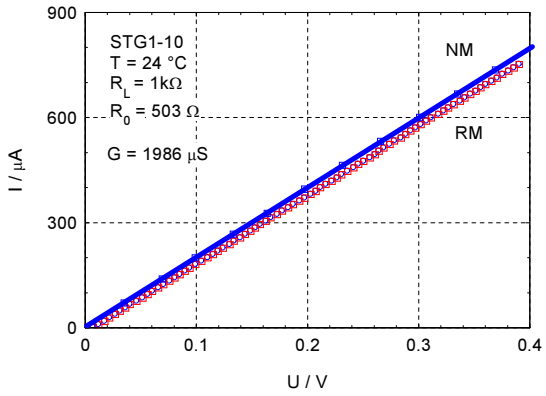

Fig. 4. The *I-V* characteristics for sample STG1-10 for NM and RM, measured at T = 24°C.

It is necessary to mention that some samples have *I-V* characteristics with resistance dependent on the electric field orientation (see Fig. 5 – results measured for sample STB1-1). In this case the *I-V* characteristics are in the first approximation linear for voltages higher than 1 V both in NM and RM giving the resistance values R_{0NM} = 4673 Ω and R_{0RM} = 7194 Ω. We suppose that these samples have a thin potential barrier formed near the contact or some cracks and/or delaminations are presented in the contact region. Such samples showed an additional g-r noise component as discussed further.

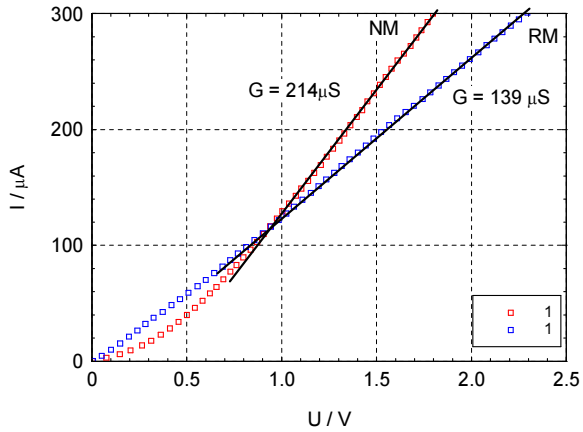

Fig. 5. The *I-V* characteristics for sample STB1-1 for NM and RM, measured at T = 24°C.

3. Electronic Noise

Our research was aimed to identify the sources of fluctuations in the sample bulk and on contacts in order to characterize its quality.

Low frequency noise was analyzed in the time and frequency domains and an excess noise, which is related to the microscopic sample structure, was studied. Fluctuation

of DC voltage on the sensor, or fluctuation of the DC current flowing through the sensor, respectively, is a measurable quantity. The experiment was performed at room temperature.

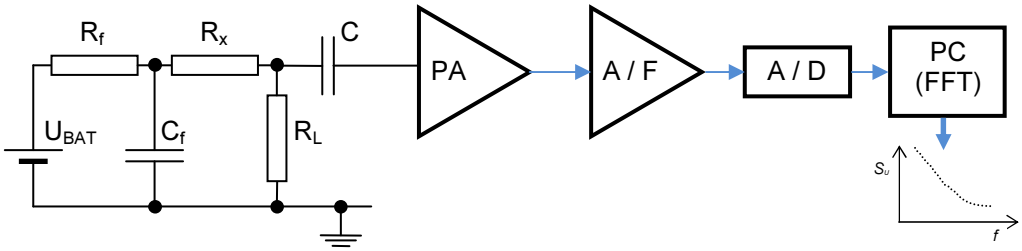

Fig. 6. Noise measurement set-up.

The low frequency noise measurement set-up is shown in Fig. 6, where R_x represents the measured sample, R_L is the load resistance, and C_f is the capacitor shunting the DC voltage source. The load resistance value was about 1 kΩ in our case. PA is the ultra-low noise voltage preamplifier (type PA15 from company 3S-SEDLAK) with the background noise spectral density of the order of 10^{-18} V^2/Hz. The pre-amplified signal passes through the band-pass filter (A/F) with a steepness of 100 dB/decade and is amplified to the required level (amplifier with band-pass filter - type AM22 from company 3S-SEDLAK). Finally, the signal is digitalized (A/D) and the noise spectrum is calculated in real time using Fast Fourier Transforms (PC-FFT). The amplifier AM22 connected with the pre-amplifier PA15 with shorted input has shown a total background noise spectral density of about 3 x 10^{-18} V^2/Hz for frequencies above 20 Hz with the $1/f^{1.3}$ noise component dominant in the frequency range below 20 Hz.

The evaluated PTC chip temperature sensor is a source of noise current. This current flows through both the measured sample and the load resistor. From the noise voltage measured on the load resistor R_L the spectral density S_{UM} is calculated. From the value of S_{UM} the spectral density S_U of the noise voltage generated by the measured sample is recalculated using the following formula:

$$S_U = (S_{UM} - S_{U0}) \cdot \frac{(R_L + R_x)^2}{R_L^2} + S_{U0}, \tag{1}$$

where S_{U0} is the measuring set-up background noise (including the device under test R_x, and load resistor R_L, for $U_{BAT} = 0$ V).

The dependence of voltage noise spectral density S_U on frequency for sample STG1-2 for a DC bias voltage of 1.7 V at a temperature of $T = 24$°C is shown in Fig. 7. The voltage noise spectral density is given by the superposition of thermal noise spectral density $S_{Uth} = 8\text{x}10^{-18}$ V^2/Hz and 1/f type noise spectral density. Noise spectral density S_U for homogeneous samples with linear *I-V* characteristics is of 1/f type in a wide frequency range and it can be described by Hooge empirical formula [16]:

$$S_U = \frac{\alpha U^2}{f N}. \tag{2}$$

Here α is a Hooge 1/f noise parameter, N is the total number of free charge carriers in the sample, f is frequency and U is the applied voltage.

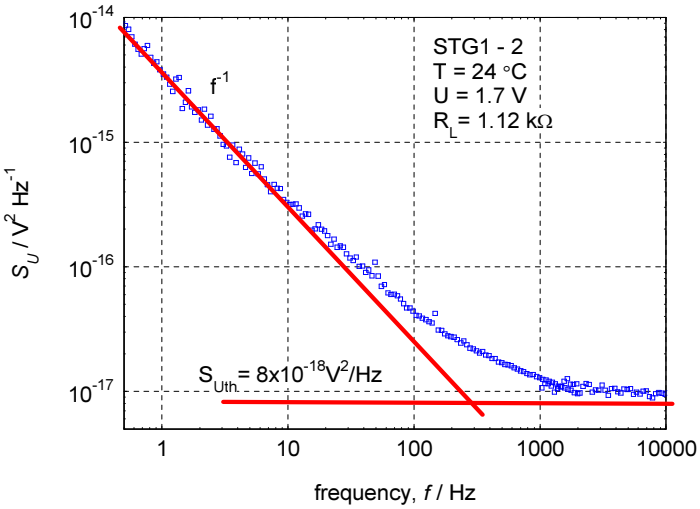

Fig. 7. Noise spectral density vs. frequency for sample STG2-1 for an applied voltage of 1.7 V, for T = 24°C and load resistance R_L = 1.12 kΩ.

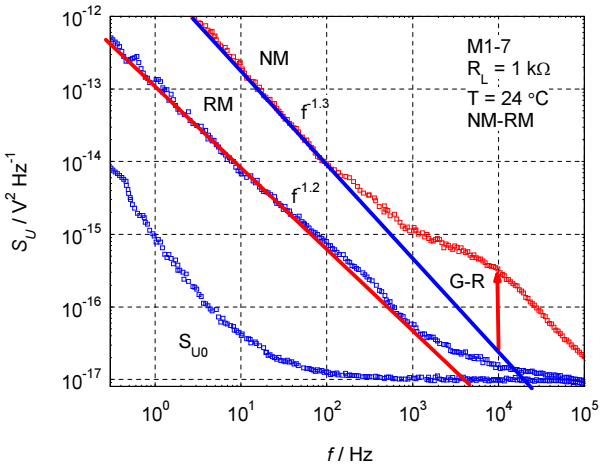

Fig. 8. Voltage noise spectral density vs. frequency for sample M1-7 for an applied voltage of 1.7 V, T = 24°C and load resistance R_L = 1 kΩ, for RM (middle curve) and NM (upper curve). The lowest curve is the measuring set-up background noise spectral density S_{U0}.

The voltage noise spectral density S_U for a sample with *I-V* characteristics dependent on the electric field orientation (as in Fig. 5) is given by the superposition of thermal noise and 1/f noise for one orientation of the electric field (Fig. 8 – the curve denoted as RM), while for the opposite orientation of electric field it is given by the superposition of thermal noise, 1/f noise and a g-r noise component (Fig. 8 – the curve denoted as NM).

The voltage noise spectral density value determined at a frequency of 1 Hz $S_{U(1\text{Hz})}$ after the subtraction of the background noise of the measuring set-up for samples STG2-1, STG2-1, and STG2-19 vs. bias voltage is shown in Fig. 9. The $S_{U(1\text{Hz})}$ value for samples STG2-1 and STG2-1 is proportional to the square of bias voltage. Such characteristics is typical for samples with homogeneous structure and ohmic contacts. The $S_{U(1\text{Hz})}$ value for sample STG2-19 increases with bias voltage with the power 2.3. A higher power of the dependence $S_{U(1\text{Hz})}$ value vs. U is often observed in the case when the defects exist in the vicinity of the contact-active layer interface.

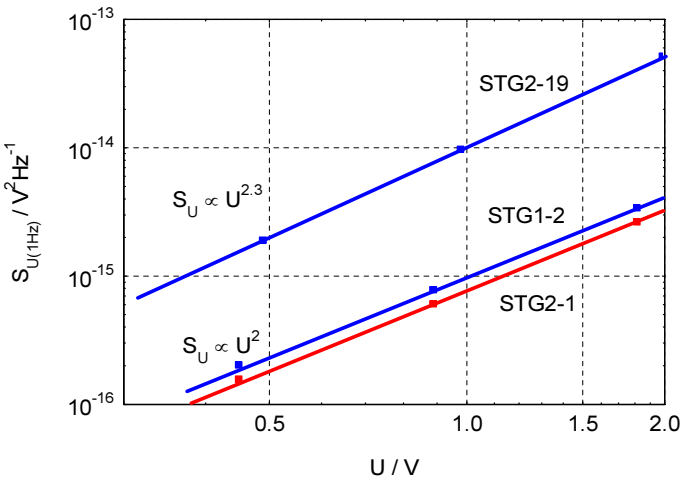

Fig. 9. The noise spectral density $S_{U(1\text{Hz})}$ at f = 1 Hz vs. bias voltage U for samples STG1-2, STG2-1 and STG2-19 after subtraction of measuring set-up background noise measured at a temperature of T = 24°C.

5. Non-Linearity of *I-V* Characteristics

The measurement of *I-V* characteristics non-linearity was performed using a Component Linearity Test Equipment from Radiometer a/s, Copenhagen NV, Denmark (CLT1). The basic measuring frequency of the pure sinusoidal signal was 10 kHz. The *I-V* characteristics non-linearity is proportional to the distortion of this pure harmonic signal and is given by the third harmonic voltage amplitude. *I-V* characteristics non-linearity measurement of two samples from the ensemble made by STG2 technology is shown in Fig. 10, where the dependence of the third harmonic voltage amplitude on the first harmonic voltage is given. We can see that the results measured for sample STG2-1 are about one order of magnitude lower comparing to the sample STG2-19. This corresponds to the noise measurements shown in Fig. 9, where $S_{U(1\text{Hz})}$ values measured for sample SRG2-19 are one order of magnitude higher comparing to the results for sample STG2-1.

The third harmonic voltage is proportional to approximately the third power of the first harmonic voltage for samples with correctly made contacts. The value of the third harmonic voltage increases with the power 2.9 in the whole range of the voltage U_1 (i.e. 0.1 to 1 V) for samples STG2-1 (see Fig. 10). The value of the third harmonic voltage increases with the power 2.8 in the range U_1 = 0.1 to 0.6 V and the power decreases for U_1 above 0.6 V for STG2-19 samples (see Fig. 10). A ratio of the third harmonic voltage to the first harmonic voltage can be used for analysis of the contact layers quality and for the homogeneity of the sample volume.

The third harmonic index (*THI*) [8, 9], expressed in dB is given by

$$THI = 20\log\left(\frac{U_3}{U_1^3}\right), \tag{3}$$

where the third harmonic voltage U_3 is expressed in microvolts and the first harmonic voltage U_1 expressed in volts.

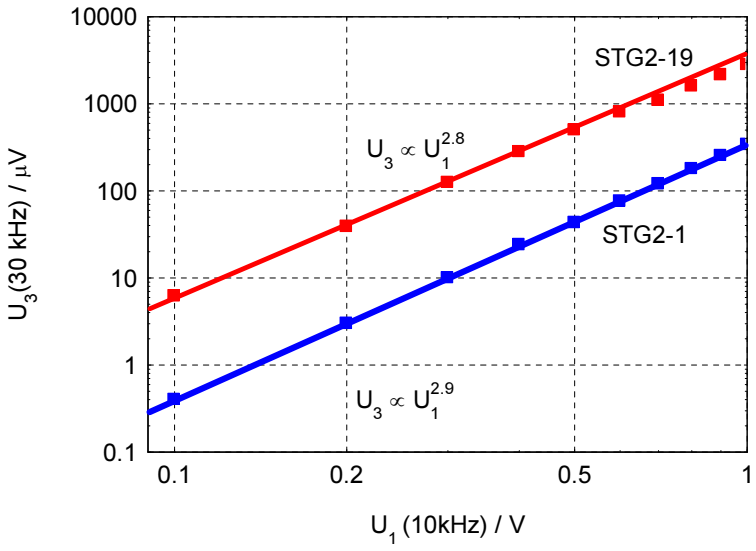

Fig. 10. The third harmonic voltage U_3 vs. the first one U_1 for samples STG2-1 and STG2-19.

The third harmonic index values calculated for all the samples of technology G (sets STG1, STG2), and technology B (sets STB1, STB2) are shown in Fig. 11, and 12, respectively. We can see that most of the samples of sets STG1 and STG2 give *THI* values in the range 50 to 60 dB, whereas only 8 parts of set STB2 fall into this range. Most of the B-technology samples give *THI* values in the range 70 to 90 dB. The third harmonic voltage value is strongly influenced by the presence of structural defects and the potential barrier or some cracks and/or delaminations in the contact region. From this point of view the G-technology can be evaluated as a technology with ohmic-type contacts. The technology G1 gives a more uniform *THI* index distribution than technology G2, which shows more samples in the range 60-70 dB.

For on-line screening of PTC chip temperature sensors by *I-V* characteristic non-linearity measurements, proper limits for the third harmonic index should be set in order to determine the parts critical from the stability point of view. From our experiments we can conclude, that the sensors giving the *THI* value higher than 60 dB could be considered as stable.

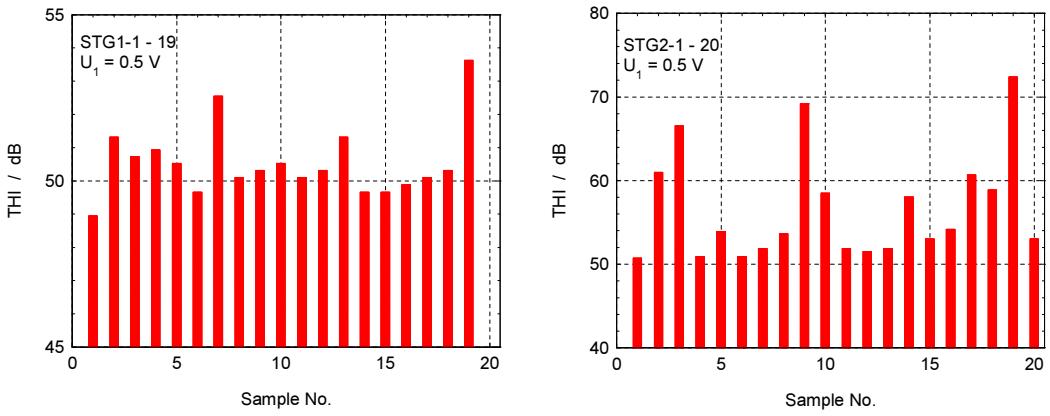

Fig. 11. The third index THI for samples of technology G – set STG1 (a) and set STG2 (b).

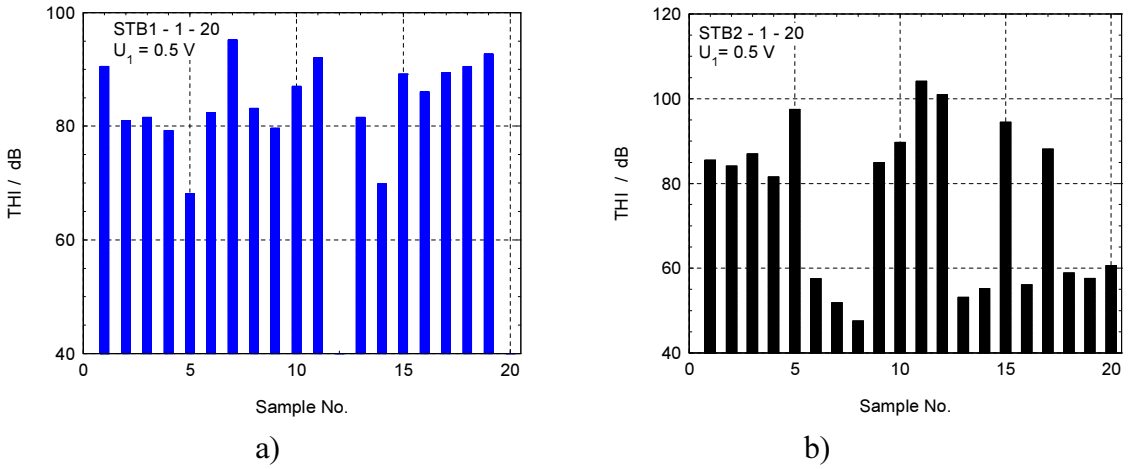

Fig. 12. The third index THI for samples of technology B – set STB1 (a) and set STB2 (b).

6. Conclusions

1. Stable resistance value and *I-V* characteristic linear and symmetrical in both bias voltage orientations represent the minimal requirements for a best quality device.
2. Spike type resistance fluctuation was observed for several sensors across the investigated ensembles. These spikes are probably a result of the surface states on the contact/active layer interface. These imperfections lead to the creation of filamentary carrier injection. The charge carriers' transport has a stochastic component which often disappears after about 24 hours of voltage application. Then the *I-V* characteristic is linear in both electric field orientations.
3. We have observed resistance fluctuation of burst noise type in some samples with non-linear *I-V* characteristics.
4. Noise spectroscopy can be used as a diagnostic tool in order to characterize the PTC chip sensors volume and contact quality and to predict the mode of possible contact failure. The low frequency noise measurements were performed in the time and frequency domains.
5. Voltage noise spectral density for samples with linear *I-V* characteristics is of 1/f type. We suppose that electron mobility and barriers between the grains are sources of these fluctuations.
6. Samples with non-linear *I-V* characteristics have a potential barrier near to the contact or some cracks and/or delaminations in the contact region and excess noise is given by the superposition of g-r and 1/f type noises.
7. Voltage noise spectral density of a sample with correctly made contacts is proportional to the square of bias voltage, while the power of dependence S_U vs. U increases for the samples with defects in the vicinity of the contact-active layer interface.
8. The value of the third harmonic voltage is lower for sensors with correctly made contacts than for the sensors with poor quality contacts. The difference was up to three orders of magnitude (60 dB). The value of the third harmonic voltage increases with the power 2.9 for samples with best quality contacts while the power decreases for sensors with poor quality contacts.
9. The third harmonic index values can be used for technology and sample quality evaluation. For the on-line screening of PTC chip temperature sensors by *I-V* characteristic non-linearity measurements, the proper limits for the third harmonic index should be set in order to determine the potentially instable components.

Acknowledgements

Research described in the paper was financially supported by the European Centres of Excellence CEITEC CZ.1.05/1.1.00/02.0068 and within the project GACR P102/11/0995 „Electron transport, Noise and Diagnostic of Schottky and Autoemission Cathodes“.

References

[1] Heywang, W. (1971). Semiconducting Barium Titanate. *J. of Material Science*, 6, 1214−1226.

[2] Saburi O. (1961). Semiconducting Bodies in the Family of Barium Titanates. *J. Amer. Ceram. Soc.*, 44, 54−63.

[3] Gerthsen, P., Groth, R., Hardtl, K. H., Heese, D., Reik, H. G. (1965). The small polaron problem and optical effects in barium titanate. *Solid State Common.* 3(8), 165−168.

[4] Zafar, S., Jones, R. E., Jiang, B., White, B., Chu, P., Taylor, D., Gillespie, S. (1998). Oxygen vacancy mobility determined from current measurements in thin $Ba_{0.5}Sr_{0.5}TiO_3$ films. *Appl. Phys. Letters*, 73, 175−177.

[5] Berglund, C. N., Baer, W. S. (1967). Electron Transport in Single-Domain Ferroelectric Barium Titanate. *Phys. Rev.*, 157, 358−366.

[6] Heywang, W. (1964). Resistivity Anomaly in Doped Barium Titanate. *J. Amer. Ceram. Soc.*, 47, 484−490.

[7] Smulko, J., Olesz, M., Hasse, L., Kaczmarek, L., Lentka, G. (2012). Problems of varistor quality assessment during exploitation. *Metrol. Meas. Syst.*, 18(2), 395−404.

[8] Kirby, P. L. (1960). The non-linearity of fixed resistors. *Electronic Engineering,* 32, 722.

[9] Fagerholt, P. O., Ewell, G. J. (2001). Third harmonic testing: An Initial Review. *Proc. CARTS - EUROPE 2001*, Copenhagen, Denmark, 221−231.

[10] Vandamme, L. K. J. (1994). Noise as a diagnostic tool for quality and reliability of electronic devices. *IEEE Transactions on Electron Devices*, 41(11), 2176−2187.

[11] Smulko, J., Darowicki, K. (2003). Nonlinearity of electrochemical noise caused by pitting corrosion. *Journal of Electroanalytical Chemistry*, 545, 59−63.

[12] Granqvist, C. G., Green, S., Jonson, E. K., Marsal, R., Niklasson, G. A., Roos, A., Topalian, Z., Azens, A., Georén, P., Gustavsson, G., Karmhag, R., Smulko, J., Kish, L.B. (2008). Electrochromic foil-based devices: Optical transmittance and modulation range, effect of ultraviolet irradiation, and quality assessment by 1/f current noise. *Thin Solid Films*, 516(17), 5921−5926.

[13] Sedlak, P., Tofel, P., Sedlakova, V., Majzner, J., Sikula, J., Hasse, L. (2011). Ultrasonic spectroscopy of silicon single crystal. *Metrol. Meas. Syst.,* 18(4), 621−630.

[14] Koktavy, B., Sikula, J. (1979). Method of Experimental Study of Fluctuation in Semiconductors. *J. Acta Phys. Slovaka*, 29, 227−236.

[15] Sikula, J. et al. (1994). 1/f Noise in Metallic Thin Films. *Proc. of 6th Quantum 1/f Noise and Other Low Frequency Fluctuations in Electronic Devices*, St. Louis, MO May 1994, *AIP Press*, 59−64.

[16] Hooge, F. N. (1969). 1/f Noise is no Surface Effect. *Phys. Lett. A*, 29, 139.